

# The formation of massive stars: accretion, disks and the development of hypercompact HII regions

Eric Keto

*Harvard-Smithsonian Center for Astrophysics, 60 Garden St., Cambridge, MA 02138*

## ABSTRACT

Observations of hypercompact HII (HCHII) regions are not easily explained by the standard model of HII regions whose dynamics and evolution are dominated by thermal or turbulent pressure, but these observations are simply understood within the contexts of more recent models – hot molecular cores, quenched HII regions, gravitationally trapped HCHII regions, photo-evaporating disks, and champagne flows – that include the gravitational attraction of embedded stars. These different theoretical models and the different observed structures of HCHII regions may be unified by a single model in which the HCHII region develops in an accretion flow that is subject to ionizing radiation. The differences in the structures of HCHII regions result from the differences in the structures of the accretion flows that form with a particular mass, gas density, and angular momentum, and the flux of ionizing radiation. The HCHII regions and some ultra-compact HII (UCHII) regions are a distinct class of HII regions whose structure, dynamics, and evolution are dominated not by pressure but by the gravitational attraction of the embedded stars and the structures associated with accretion.

*Subject headings:* stars: early type — stars: formation — ISM: HII regions

## 1. Introduction

In areas of active massive star formation, high angular resolution radio observations detect clusters of tiny HII regions with size scales small enough that the escape velocity from the stars equals or exceeds the sound speed of the ionized gas throughout the volume of the HII regions. It is on these size scales that the gravitational attraction of the stars dominates the thermal pressure of the ionized gas, and on these size scales it is possible for an accretion flow to pass through an HII region. The hypercompact HII (HCHII) regions,

which are the smallest and therefore the youngest of the HII regions, may therefore be associated with massive stars still in formation with active accretion processes. The HCHII regions have four observational characteristics that are difficult to explain with models of HII regions in which the dynamics are dominated by the thermal or turbulent pressure of the ionized gas, but are easily understood with models that include the gravitational attraction of the stars and accretion processes. The first of these observational properties is a characteristic morphology that shows a small bright region within a much larger extent of low level continuum emission. Pressure forces should smooth out any density inhomogeneities within the HII region, but observations indicate strong density contrasts between regions of different size scale. Second, the radio continuum emission from many HCHII regions has a spectral index that scales with frequency approximately as  $\nu^1$  over several decades in frequency, intermediate between the optically thick,  $\nu^2$ , and optically thin,  $\nu^{-0.1}$ , limits expected for HII regions of uniform density. Third, the spectra of radio recombination lines often show supersonic line widths. These broad lines indicate gas velocities and densities (pressure broadening) that exceed the predictions of models dominated by thermal pressure. In pressure-driven expansion the maximum gas velocity is approximately the sound speed, and the densities, if high enough to cause the observed pressure broadening, would result in optically thick spectral indices. Fourth, the radio recombination line spectra often have complex line profiles that indicate complex flows of ionized gas within the HII regions and not the simple outward motion of pressure-driven expansion. In some cases, observations of radio recombination lines with sufficient spatial resolution are able to directly map inflows and outflows within HII regions. The observation of inward flowing ionized gas is directly contradictory of pressure driven expansion. This article explores how the HCHII regions and their observational characteristics may be understood within the context of a simple model in which the HCHII region is the ionized portion of an accretion flow. Depending on the properties of the accretion flow, the HCHII region may appear as a gravitationally trapped HII region, an ionized accretion flow, or a photo-evaporating disk.

## 2. Observational characteristics

### 2.1. Morphology

The HCHII regions are often seen as bright substructures within a larger extent of ionized gas (Kurtz et al 1999; Kurtz 2000; Kim & Koo 2001; Ellingsen et al. 2005; Depree et al. 2005). Figure 1, the continuum image of the HCHII region GAL 035.20-1.7, shows the difference in scale and brightness between the arcsecond HCHII region and the arcminute extended emission. Such a strong density contrast cannot be explained by models of HII

regions dominated by the thermal pressure of the ionized gas (e.g. Spitzer 1978) because pressure forces should smooth out any density fluctuations inside the HII region within a sound crossing time. However, the structure has a simple interpretation if the bright emission is from gas whose high density gas is maintained by the gravitational field of the star or stars while the extended emission is from gas outside the gravitationally dominated zone that has a lower and more uniform density.

Because the gravitational field of the stars decreases rapidly with distance as  $r^{-2}$ , only a small volume around the star is gravitationally dominated. In the case of GAL 035.20-1.7, the width (FWHM) of the HCHII of 3" corresponds to 0.04 pc at 3.1 kpc. If the gravitational radius,  $R_g$  is of this scale, then the implied gravitational mass is about  $1000 M_\odot$ . This large mass implies that the source powering the HCHII region is a small group rather than a single massive star.

## 2.2. Intermediate spectral indices

Other evidence for the effects of stellar gravity within HCHII regions is found in the spectral index of the observed radio continuum emission. The HCHII regions often show a spectral index scaling approximately linearly over decades in frequency (Hofner et al. 1996; Franco et al. 2000; Testi et al. 2000; Kurtz et al 2001; Beuther et al 2004; Ignace & Churchwell 2004). This proportionality over this large frequency range cannot be explained by the constant density of a pressure dominated HII region. However, intermediate spectral indices are easily produced with various combinations of optically thick and thin emission blended within the observing beam as would be the case if the HII region had a strong internal density gradient. This blending stretches the "knee" of the transition region over a large enough frequency range that the continuum emission appears to have a scaling intermediate between the optically thick and thin limits (Keto 2003).

Because there are a number of ways to stretch the spectral index, for example by random density fluctuations (Ignace & Churchwell 2004), or the addition of continuum emission from dust or a stellar wind (Testi et al. 2000), the observation of an intermediate spectral index does not unambiguously implicate a density gradient produced by stellar gravity. However, stellar gravity must produce a density gradient in the gas around the star, and that density gradient alone is sufficient to explain the intermediate spectral indices observed at cm wavelengths in HII regions that are small enough for gravitational forces to be significant.

### 2.3. Supersonic line widths

The HCHII regions are observed to have radio recombination line widths several to many times the thermal width (Zijlstra et al. 1990; DePree et al. 1994; Keto et al. 1995; Hofner et al. 1996; Johnson et al 1998; Jaffe & Martin-Pintado 1999; Keto 2002a; Sewilo et al. 2004; Keto & Wood 2006). Supersonic line widths are difficult to explain in the model of a pressure-dominated, constant-density HII region because the gas is expected to expand at a velocity not exceeding the sound speed. However, the supersonic line widths are easily explained as a combination of supersonic dynamics inside the HII region and pressure broadening in the high densities produced by the density gradients that are maintained by stellar gravity. If the gas dynamics are dominated by gravitational forces such that the pressure forces are irrelevant, then the gas motions must be supersonic. Such motions are inevitable in the gravitational field around a star or group of stars. Not only must there be a density gradient in the surrounding gas, but the gas must be in motion, either infalling toward the star or expanding outward (Shu 1992, pg 80).

In considering the flows in ionized gas it is important to keep in mind that supersonic motions can be associated with outflowing gas in bipolar outflows or champagne flows (Keto et al. 1995; Shu 1992) as well as with the inflowing gas of an accretion flow. Bipolar outflows are invariably associated with accretion which implies a dominance of inward gravitational forces over thermal pressure. Champagne flows are associated with steep density gradients ( $n \sim r^\alpha$  with  $\alpha < -3/2$ ) that are not found in models of pressure dominated HII regions. Thus bipolar outflows and champagne flows may also be thought of as associated with the gravitational field of the stars.

This broader definition of gravitationally dominated HII regions that includes HII regions with outflows expands on the suggestion of Keto (2003) that HCHII regions are ionized accretion flows. This earlier definition seems too restrictive to explain all the various morphologies of observed HCHII regions. In this article, section 4 explains how the ionization of accretion flows can produce a variety of HCHII regions, some with high velocity outflows, depending on the structure of the accretion flow.

## 3. The three R's of HCHII regions

One standard model for an accretion flow describes the motion of the gas as if on ballistic trajectories around a point mass (Ulrich 1976; Terebey, Shu & Cassen 1984, U76, TSC84). This accretion model depends on three parameters, the central mass, the density at infinity, and the initial angular momentum. When considering HCHII regions and ionized accretion

flows the flux of ionizing photons should be added to this set of three parameters. The ionizing flux is independent of the central mass if the HCHII region contains more than one star. This set of four parameters can be organized into three characteristic radii, the gravitational or Bondi radius  $R_g = GM/2c^2$ , the radius of disk formation  $R_d = \Gamma^2/GM$ , where  $\Gamma$  is the specific angular momentum (U76), and the radius of ionization equilibrium,  $R_i$ . Different combinations of parameters, result in accretion flows and HCHII regions with different structures. Of particular interest are those that match other concepts of HCHII regions, the photoevaporating accretion disks of Hollenbach et al. (1994); Lizano et al. (1996); Johnstone, Hollenbach, & Bally (1998); Lugo, Lizano & Garay (2004), the ionized accretion flows of Keto (2002b, 2003)), and the champagne flows of Shu et al. (2002). This section discusses the interpretation of the three characteristic radii, the three  $R$ 's of HCHII regions.

### 3.1. $R_i$ , the radius of ionization equilibrium

In the simplest conception, ionization equilibrium within an HII region is set by the rate of ionizing photons from the stars and the rate of recombination in the ionized gas. The recombination rate is a function of the square of the ionized gas density which in the U76-TSC84 model is set by the conservation of mass and the prescribed density at infinity.

### 3.2. $R_g$ , The gravitational radius

In an accretion flow that passes from a molecular to an ionized state the gas pressure increases by approximately two orders of magnitude. This increase in pressure results in an outward force that can be competitive with the inward force driving the accretion. However, the U76-TSC84 accretion model of ballistic trajectories does not consider the thermal pressure of the gas. To understand the relationship between the gravitational radius,  $R_g$ , and the radius of ionization,  $R_i$ , it is instructive to consider a model for accretion that includes the thermal pressure of the accreting gas along with the gravitational energy. The simplest such model is that of isothermal spherical accretion with the velocities of the flow determined by the Bernoulli equation along streamlines (Bondi 1952).

In the well-known solution of the Bernoulli equation that has boundary conditions appropriate for accretion, the flow passes through a transonic point at  $R_g = GM/2c^2$  that divides the accretion flow into an inner and outer region that are dominated by gravity and thermal pressure respectively. At radii less than  $R_g$  the flow velocities are supersonic, and the velocity and density structure approximates a free-fall solution. Pressure forces at

$r < R_g$  are negligible. At larger radii, the flow is subsonic, and the density structure of the flow approximates a hydrostatic solution with pressure forces approximately in balance with gravitational forces. If the ionizing flux from the stars and the density of the accretion flow are such that  $R_i < R_g$ , where the sound speed is that of the ionized gas, then the ionization front may persist as a static front (R-type) within the infalling gas (Keto 2002b). If  $R_i > R_g$ , then the pressure of the ionized gas in the region beyond  $R_g$  exceeds the inward gravitational force and the ionized gas may flow outward.

### 3.3. $R_d$ , the spin-up of accretion and disk formation

The observations of the accretion flow around G10.6–0.4 show that the flow is quasi-spherical on larger scales as seen in the molecular gas (Keto 1990; Sollins et al. 2005) and spins-up to form a disk at smaller scales as seen in the ionized gas. The transition from a quasi-spherical to disk-like structure is well described by the U76-TSC84 model in which the gas conserves angular momentum. The transition occurs at the radius where the centrifugal force equals the gravitational force,  $\Gamma^2/r_d^3 = GM/r_d^2$ . The radius of disk formation can also be written in a form analogous with the gravitational radius as  $R_d = GM/v_\phi^2$  where  $v_\phi$ , the orbital velocity at  $R_d$ , replaces the sound speed. In the U76-TSC84 model,  $R_d$  depends on the angular momentum of the flow at infinity and thus may be taken as a property of the cloud in which the accretion flow develops.

## 4. The different structures of HCHII regions

Different combinations of the relative values of  $R_g$ ,  $R_i$ , and  $R_d$  result in HCHII regions with different structures. Of particular interest are those combinations that result in structures that match either observed HCHII regions or one of several theoretical models of HCHII regions. For example, if  $R_d > R_g > R_i$  the flow has a relatively high angular momentum such that a disk or torus forms outside the HII region in the molecular phase of the flow. Observations such as those of G10.6–0.4 that show the formation of a disk within the HII region indicate a flow of relatively low angular momentum such that  $R_d < R_i \leq R_g$ . The theoretical model of a photo-evaporating molecular disk (Hollenbach et al. 1994; Lizano et al. 1996; Johnstone, Hollenbach, & Bally 1998; Lugo, Lizano & Garay 2004) suggests a relatively high angular momentum to produce a disk in the molecular portion of the flow and a relatively high flux of ionizing radiation to extend the HII region around the molecular disk,  $R_i \geq R_d > R_g$ .

In the following sections are illustrations of six cases, half with large  $R_d$  (high angular momentum) compared to  $R_i$  and  $R_g$  and half with small  $R_d$  (low angular momentum) each constructed with three levels of ionization. These different realizations show how apparently different structures that are observed or envisioned in theoretical HCHII regions are related to one basic model.

#### 4.1. Individual models

##### 4.1.1. *Gravitationally trapped HII regions with thick molecular disks*

The first case, figure 2, shows a high angular momentum, low luminosity flow that forms a disk in the molecular portion of the accretion flow. Because the radius of disk formation is not an actual boundary, flattening of the flow begins at some distance outside  $R_d$  and increases progressively inward. In such a flow the spherical volume between  $R_d$  and  $2R_d$  contains several times the mass that is within  $R_d$ . Thus we would expect that observations that are straining for angular resolution and sensitivity would pick up the greater volume and mass of the gas outside  $R_d$  where the flow is not yet fully flattened into a disk. The structure seen in such an observation would resemble a thick disk or torus rather than a thin accretion disk. Thus observations of thick molecular torii (Cesaroni et al. 1997; Hofner et al. 1999; Beltran et al. 2005; Zhang et al. 1998, 2002; Kumar et al. 2003; Chini et al. 2004) may be observations of the outer regions of a standard star forming accretion flow that is beginning to spin-up into a disk. In these flows, the HCHII region may be "quenched" (Walmsley et al 1995) or if the ionizing luminosity is such that  $R_i < R_g$ , gravitationally trapped (Keto 2002b), perhaps still quite small in size, optically thick in the centimeter continuum and difficult to detect in VLA surveys. If the HII region is undetectable, the molecular gas may look like a hot molecular core.

##### 4.1.2. *Bipolar HCHII regions*

If the same flow as in the preceding example is subjected to a higher ionizing luminosity then the boundary of the HII region is at a greater distance, but because of the higher density in the mid-plane of the accretion flow, the extent is larger along the rotation axis. Examples of HCHII regions that appear bipolar are K3-50A (DePree et al. 1994) and a few in Sgr B2 (Depree et al. 2005). Bipolar HII regions are a minority of the HCHII regions. In the surveys of Wood & Churchwell (1989) and Kurtz et al. (1994) there is, for example, no category for bipolar HII regions. This may be because there is a limited range of ionizing

flux that results in this morphology. In contrast there is a large range of low ionizing flux that produces "quenched" HCHII regions or hot molecular cores and a large range of high ionizing flux that produces photo-evaporating disks as shown in the next example.

#### 4.1.3. *Photo-evaporating disks*

Starting with the same accretion flow as in the two previous examples, and increasing the ionizing flux further results in a model similar to the photo-evaporating disks of Hollenbach et al. (1994); Lizano et al. (1996); Johnstone, Hollenbach, & Bally (1998); Lugo, Lizano & Garay (2004). In this model, the high ionizing flux produces an HII region that has over-run the molecular disk, figure 2. Because much of the disk is beyond  $R_g$ , the ionized gas is not gravitationally bound and flows away from the disk. The outflowing gas is replaced by evaporation off the disk. Only a small region around the star is within  $R_g$  and able to accrete ionized gas. The U76-TSC84 model does not have the capability to describe the structure of the outflow off the disk, but the significance of this simple accretion model is that it shows how the photo-evaporating disks are related to the other models of HCHII regions through the relative sizes of  $R_g$ ,  $R_d$ , and  $R_i$ .

#### 4.1.4. *Gravitationally trapped HII regions with a quasi-spherical molecular flow*

Now we shift to the low angular momentum flows. In this example, as in the first example, section 4.1.1, the HII region is contained entirely within the Bondi radius so that the molecular accretion flow passes through the ionization boundary and continues on to the star as an ionized accretion flow. In this case,  $R_g > R_d$ . However because the density of the flow scales with  $R_g$ , then relative to example 1, the density becomes high before the flow has flattened into a disk. (In all cases,  $R_g$  is computed with the sound speed of the ionized gas.) Thus an observation of this structure would show a structure very similar to example 1, section 4.1.1, but with a more strongly flared or thicker molecular disk or torus or even quasi-spherical in the limit of very low angular momentum (small  $R_d$ ).

#### 4.1.5. *Bipolar HII regions with flared molecular disks*

Starting with the same accretion flow as in example 4 and increasing the ionizing radiation results in a bipolar HII region with a strongly flared or very thick molecular disk. This case is very similar to that of example 2, but because of the lower angular momentum the

molecular flow is more flared and thicker than in example 2, section 4.1.2, and therefore the HII region is more strongly bipolar. In figure 3, the HII region is unbounded in the direction of the rotation axis as a result of the level of the ionizing flux in this example. Nonetheless, because the continuum emission scales as the square of the electron density which is falling off sharply with distance from the center of the flow, an observation would show a bipolar HII region of limited extent with a width at half-maximum at the distance where the electron density has fallen to  $\sqrt{2}$  of the peak.

#### 4.1.6. *Ionized accretion disks*

Finally with a high luminosity we find a fully ionized disk entirely within the gravitational radius. Because  $R_d < R_i < R_g$  the flow does not flatten into an accretion disk until entirely within the HII region. Thus the disk forms out of fully ionized gas. At the high densities along the mid-plane of the disk, the gas may recombine to become atomic or molecular. Thus the disk itself is not expected to be fully ionized throughout its volume. The significant difference between this structure and the photo-evaporating disks of example 3 (section 4.1.3) is that here the flow of ionized gas is inward and onto the disk whereas in the case of the photo-evaporating disk of example 3 the flow is outward and off the disk. There is one very well documented example of this type of structure, G10.6–0.4 (Keto 1990; Keto 2002b; Sollins et al. 2005; Keto & Wood 2006).

#### 4.1.7. *Champagne flows*

Champagne flows form wherever the density gradient in the gas surrounding an ionizing star is steeper than  $r^{-3/2}$ . While the density gradients in the U76-TSC84 model are always less steep, this is a characteristic of this particular model. Accreting massive stars may be surrounded by molecular clouds or cloud cores that have density gradients that are steeper than  $r^{-3/2}$  in some direction. If so a champagne flow forms in this direction, but accretion may still continue into the HII region from other directions. As pointed out in Shu et al. (2002), the gas in a champagne flow must be replenished if the flow is to have a lifetime longer than a crossing time. An accretion flow from another direction may be the source of this replenishment. Champagne flows are common among HCHII regions, but are not included in the models calculated here because they are not well described by the density and velocity model of the U76-TSC84 accretion flow.

## 5. Conclusions

A simple model of an accretion flow that is subject to ionizing radiation is able to provide a variety of structures depending on the values of several parameters that describe the flow. These structures match those that are taken as the starting points in more detailed models of HCHII regions, quenched HII regions (Walmsley 1995), hot molecular cores, gravitationally trapped HII regions (Keto 2002b, 2003), photo-evaporating disks (Hollenbach et al. 1994; Lizano et al. 1996; Johnstone, Hollenbach, & Bally 1998; Lugo, Lizano & Garay 2004), and champagne flows (Keto et al. 1995; Shu et al. 2002). With the exception of the model for champagne flows, these models are all models of accretion flows, and in the model for champagne flows, it is the gravitational attraction of the star that sets up the steep density gradient required for a champagne flow. Thus the HCHII regions are all HII regions whose structure, dynamics, and evolution are dominated by the gravitational attraction of the stars and the accretion flows of high mass star formation.

## A. Appendix

## B. Methods

There are six different models presented in the figures. All models have the same central mass, is  $100 M_{\odot}$ . With sound speeds  $0.6 \text{ kms}^{-1}$  and  $12.9 \text{ kms}^{-1}$ ,  $R_g(\text{ion}) = 218 \text{ AU}$  and  $R_g(\text{mol}) = 0.7 \text{ pc}$ . The radii,  $R_g$  and also  $R_d$ , simply scale linearly with the mass. The first three models have high angular momentum while the last three are low angular momentum, with rotational velocities of  $0.5 \text{ kms}^{-1}$  and  $1.5 \text{ kms}^{-1}$  respectively, both at a radius of  $0.02 \text{ pc}$ . This corresponds to  $R_d(\text{high}) = 0.00208 \text{ pc}$  (428 au) and  $R_d(\text{low}) = 0.00023 \text{ pc}$  (47 au).

For each of these two cases of angular momenta there are 3 flux levels of ionizing flux that are chosen to produce a small HCHII region, a bipolar HCHII region, and a broadly ionized region around the accretion flow. For the accretion flow with high angular momentum, the fluxes of ionizing radiation are  $1 \times 10^{48}$ ,  $3 \times 10^{49}$ ,  $5 \times 1.5^{50}$  photons  $\text{s}^{-1}$ , and for the low angular momentum flow,  $1 \times 10^{46}$ ,  $5 \times 10^{46}$ ,  $5 \times 10^{47}$  photons  $\text{s}^{-1}$ .

The boundary of the HII region is the point where the flux of ionizing photons falls to zero,  $S(R_i) = 0$ . For a spherical HII region (Spitzer 1978, eqn. 5.20),

$$\int_{r_0}^{R_i} \frac{dS(r)}{dr} = S(R_i) - S(r_0) = - \int_{r_0}^{R_i} 4\pi r^2 n_e^2(r) \alpha^2 dr$$

where  $r_0$  is the inner boundary of ionization which may be the boundary of the star,  $S(r_0)$  is the ionizing flux at this point,  $n_e$  is the electron density, and  $\alpha$  is the recombination rate.

Although the model accretion flows with angular momentum are not spherical, this equation may be used as an approximation to find the radius of ionization equilibrium,  $R_i$ , along any outward ray from the star. The electron density along the ray is set by the structure of the accretion flow.

Because the U76-TSC84 model does not include gas pressure, the flow in this model cannot be reversed by ionization. Therefore it is necessary to indicate the direction of flow after the calculation of the ionization boundary. This is simply done in the illustrations by reversing the direction of flow if the gas is both ionized and outside of  $R_g$ .

The U76-TSC84 model also does not include a bipolar outflow. An arbitrary bipolar outflow is therefore added to the models. The opening angles of the bipolar outflows are set to  $10^\circ$ ,  $20^\circ$ ,  $30^\circ$  for the three levels of ionizing flux. The velocity in the bipolar outflow is set to scale linearly with distance, the velocity is the sound speed at  $R_g$ , and the density decreases as  $r^{-3}$  as appropriate for mass conservation in a bipolar outflow flow with this density profile.

## REFERENCES

Beltran, M.T., Cesaroni, R., Neri, R., Codella, C., Furuya, R.S., Testi, L., Olmi, L., 2005, AA, 435, 901

Beltr'an, M. T., Cesaroni, R., Neri, R., Codella, C., Furuya, R. S., Testi, L. & Olmi, L. 2004, ApJ, 601, L187

Beuther, H., Zhang, Q., Greenhill, L.J., Reid, M.J., Wilner, D., Keto, E., Marrone, D., Ho, P.T.P., Moran, J.M., Rao, R., Shinnaga, H., Liu, S.-Y., 2004, ApJL, 616, L31

Bondi, H., 1952, MNRAS, 112, 195

Cesaroni, R., Felli, M., Testi, L., Walmsley, C.M., Olmi, L., 1997, AA, 325, 725

Chini, R., Hoffmeister, V., Kimeswenger, S., Nielbock, M., Nurnberger, D., Schmidtobreick, L. & Sterzik, M., 2004, Nature, 429, 155

DePree, C.G., Goss, W.M., Palmer, P., Rubin, R., 1994, 428, 670

DePree, C.G., Wilner, D.J., Deblasio, J., Mercer, A.J., Davis, L.E., 2005, ApJL, 624, L101

Ellingsen, S.P., Shabala, S.S., Kurtz, S.E., 2005, MNRAS, 357, 1003

Hofner, P., Kurtz, S., Churchwell, E., Walmsley, C. & Cesaroni, R., 1996, ApJ, 460, 359

Hofner, P., Cesaroni, R., Rodriguez, L.F., Marti, J., 1999, 345, L43

Franco, J., Kurtz, S., Hofner, P., testi, L., Guillermo, G.-S., Martos, M., 2000, ApJL, 542, L143

Hollenbach, D., Johnstone, D., Lizano, S., Shu, F., 1994, ApJ, 428, 654

Ignace, R., Churchwell, E., 2004, ApJ, 610, 351

Jaffe, D.T. & Martin-Pintado, J., 1999, 520, 162

Johnson, C.O., DePree, C.G., Goss, W.M., 1998, ApJ, 500, 302

Johnstone, D., Hollenbach, D., & Bally, J., 1998, ApJ, 499, 758

Keto, E., 1990, ApJ, 355, 190

Keto, E., Welch, W., Reid, M., Ho, P., 1995, ApJ, 444, 765

Keto, E., 2002a, ApJ, 568, 754

Keto, E., 2002b, ApJ, 580, 980

Keto, E., 2003, ApJ, 599, 1196

Keto, E. & Wood, K., 2006, ApJ, 637, 850

Kim, K.T., Koo, B.C., 2001, ApJ., 549, 979

Kumar, M., Fernandez, A., Hunter, T., Davis, C., Kurtz, S., 2003, AA, 412, 175

Kurtz, S., Churchwell, E., Wood, D.O.S., 1994, ApJS, 91, 659

Kurtz, S., Watson, A.M., Hofner, P., Otte, B., 1999, ApJ, 514, 232

Kurtz, S., 2000, RevMexAA, 9, 169

Kurtz, S., Franco, J., Garcia-Barreto, J.A., Hofner, P., Guillermo, G.-S., Fuente, E., Esquivel, A., 2001, RevMexAA, 10, 45

Lizano, S., Canto, J., Garay, G., Hollenbach, D., 1996, ApJ, 465, 216

Lugo, J., Lizano, S., Garay, G., 2004, ApJ, 614, 807

Sewilo, M., Churchwell, E., Kurtz, S., Goss, W.M., Hofner, P., 2004, ApJ, 605, 285

Sollins, P., Zhang, Q., Keto, E., Ho, P., 2005, ApJ, 624, L49

Shu, F., 1992, The Physics of Astrophysics, Volume II, Gas Dynamics, University Science Books, Mill Valley, CA

Shu, F., Lizano, S., Galli, D., Canto, J., Laughlin, G., ApJ, 2002, 580, 969

Spitzer, L., Jr., 1978, Physical Processes in the Interstellar Medium, (New York:Wiley)

Terebey, S., Shu, F., Cassen, P., 1984 ApJ, 286, 529

Testi, L., Hofner, P., Kurtz, S., & Rupen, M., 2000, AA, 359, L5

Ulrich, R., 1976, ApJ, 210, 377

Walmsley, M., 1995, Revista Mexicana de Astronomia y Astrofisica Serie de Conferencias, Vol. 1, Circumstellar Disks, Outflows and Star Formation, Cozumel, Mexico, Nov 28-Dec 2, 1994, p. 137

Wood, D.O.S., Wood & Churchwell, E., 1989, ApJS, 69, 831

Zhang, Q., Hunter, T., Sridharan, T., 1998, ApJ, 505, 151

Zhang, Q., Hunter, T., Sridharan, T., Ho, P., 2002, ApJ, 566, 982

Zijlstra, A.A., Pottasch, S.R., Engels, D., Roelfsema, P.R., te Lintel Hekkert, P., Umana, G., MNRAS, 1990, 246, 217

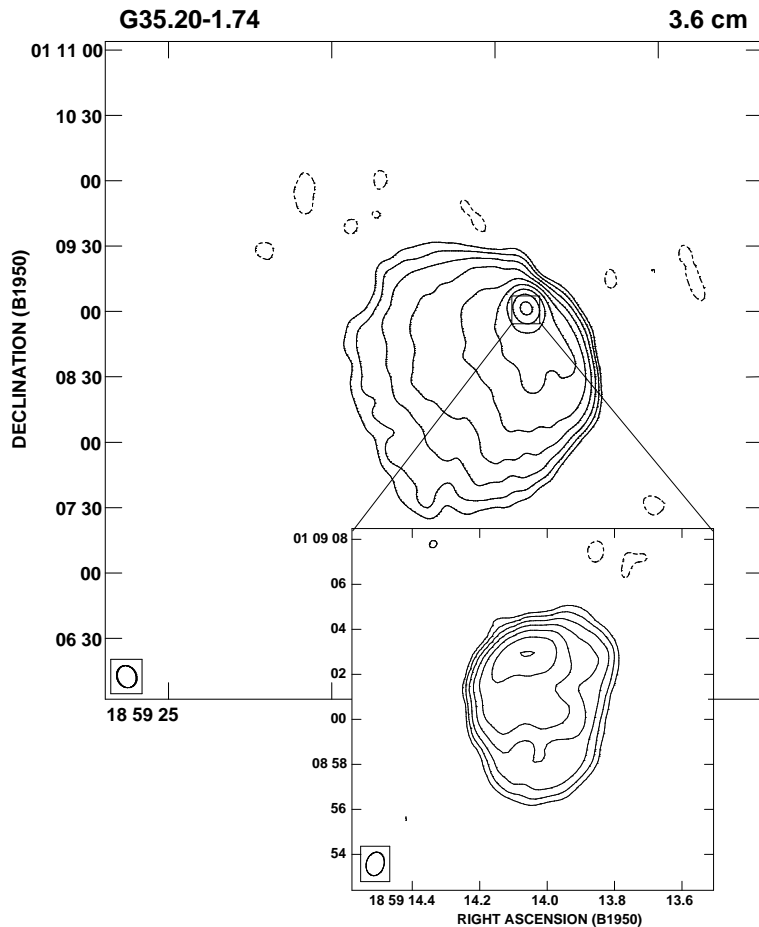


Fig. 1.— The HII region GAL 035.20-1.7 in the 3.6 cm radio continuum showing the typical morphology of an HCHII region (from Kurtz (2000)). The HCHII region is the small, bright peak surrounded by low level extended emission. The peak emission in the upper image is 2.48 Jy/beam with contours in 3dB steps starting from 8 mJy/beam. The peak emission in the inset image is 0.173 Jy/beam with contours in 3dB steps starting with 0.242 mJy/beam.

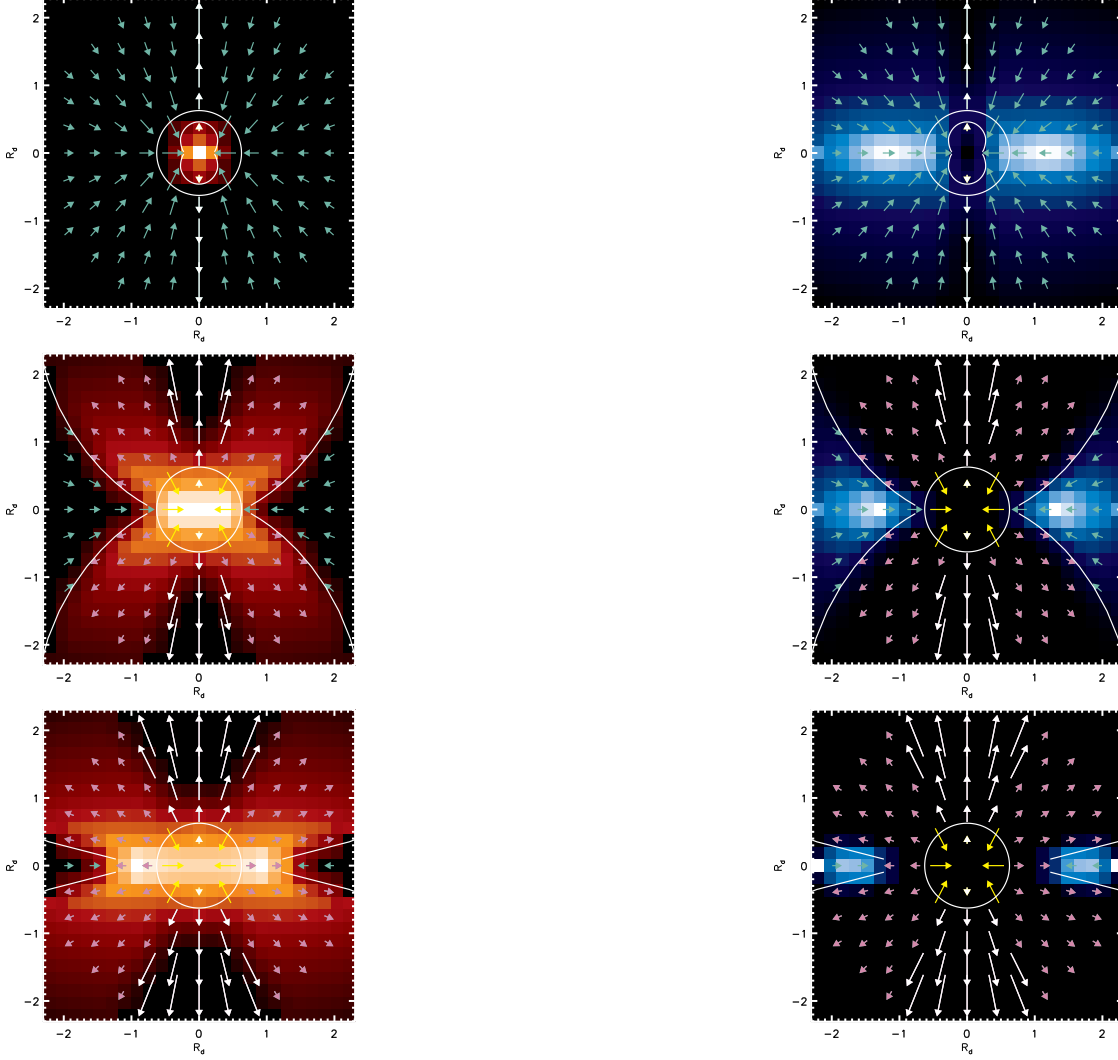


Fig. 2.— Model of a high angular momentum accretion flow subject to 3 levels of ionizing radiation. The models correspond to *top*: quenched or gravitationally trapped HII region within a molecular disk (text section 4.1.1), *middle*: a bipolar HII region with a molecular disk (text section 4.1.2), *bottom*: a photo-evaporating disk (text section 4.1.3). Model details described in appendix. *Left*: ionized gas. *Right*: molecular gas.

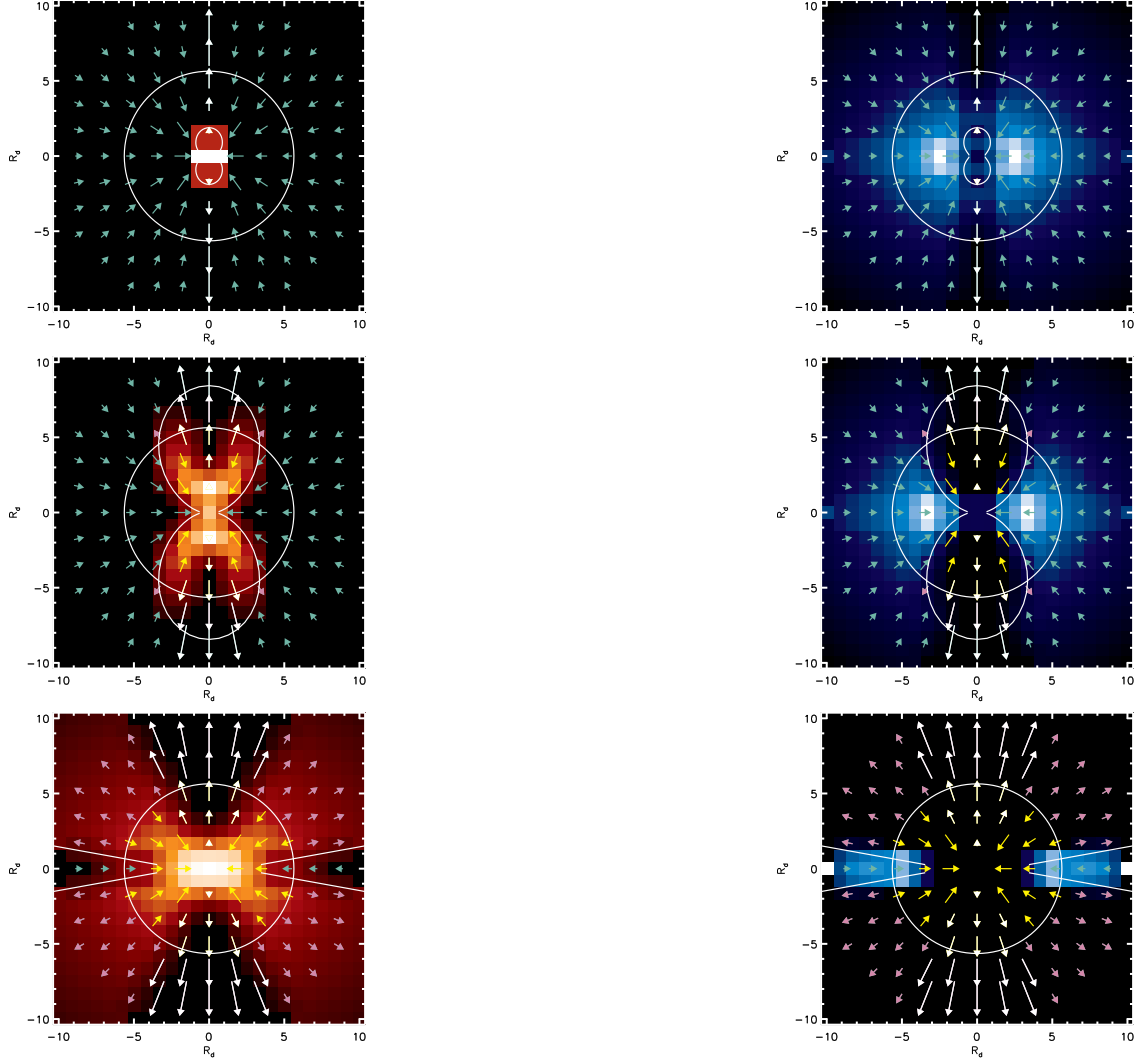


Fig. 3.— Model of a low angular momentum accretion flow subject to 3 levels of ionizing radiation. The models correspond to *top*: quenched or gravitationally trapped HII region within a thick molecular disk or torus (text section 4.1.4), *middle*: a bipolar HII region with a flared molecular disk or torus (text section 4.1.5), *bottom*: an ionized accretion flow (text section 4.1.6). Model details described in appendix. *Left*: ionized gas. *Right*: molecular gas.